Global Journal of Health Science; Vol. 9, No. 9; 2017
ISSN 1916-9736 E-ISSN 1916-9744
Published by Canadian Center of Science and Education

Finite Element Analysis of Screw-Tightening Torque Applied to Custom and Conventional Abutment

Sang Hyun Lee[1,2], Kyu Bok Lee[1,2] & Min Ho Hong[1,2]

[1] School of Dentistry, Kyungpook National University, Daegu, Republic of Korea

[2] Advanced Dental Device Development Institute, Kyungpook National University, Daegu, Republic of Korea

Correspondence: Kyu Bok Lee, School of Dentistry, Kyungpook National University, 2177 Dalgubuldaero, Jung-gu, Daegu, 41940, Republic of Korea. Tel: 053-600-7674. E-mail: kblee@knu.ac.kr

Received: July 7, 2017 Accepted: August 21, 2017 Online Published: August 28, 2017

doi:10.5539/gjhs.v9n9p165 URL: https://doi.org/10.5539/gjhs.v9n9p165

Abstract

The aim of this study was to design an abutment with an esthetic emergence profile contour using CAD technology and compare the stress distribution within the structure between the custom abutment and conventional abutment according to the screw tightening torque using 3D finite element analysis (FEA). The maximum tensile principal stress was found in the endpoint of the screw head and the start point of the screw line with regard to the application of the tightening torque of the screw. A similar pattern was observed in all of the following screws: 10N·cm, 20N·cm, and 30N·cm. The tightening torque of the screw had a significant impact on the changes in the stress of the abutment and screw fixture. This study also found that the condition in which the screw load was applied showed a more realistic description of the behavior of a single fixed dental implant than the condition in which the screw load was not applied. This study examined the optimal tightening torque value of the screw for the denture used in this study at a location slightly higher than 20N·cm. The difference in the custom abutment and conventional abutment did not have a significant impact on the supporting bone with regard to the external load. In regard to the stress occurring in the screw, the custom abutment had a lower degree of stress than the conventional type. Therefore, a screw fracture would occur less frequently in a custom abutment than a conventional abutment.

Keywords: custom abutment, CAD/CAM System, Finite Elements Analysis

1. Introduction

As implant prostheses have become more generalized, there has been a significant increase in aesthetic interest. Accordingly, it is important to continuously solve the issues of producing functionally excellent and aesthetically successful implants. Because the small diameter and uniform round shape of the fixture are different from the form of the tooth root of natural teeth, it is difficult to produce a crown in the form of lost natural teeth, and there are issues regarding the design of the abutment structure that supports a restoration (Bichacho, 1998; Ting, Wenhe, Ning, & Chunbo, 2010). The conventional abutment used in the fixture restoration is standardized, and the ease of use and suitability is excellent. On the other hand, there is a limitation in applying conventional abutments to all clinical cases. In other words, the use of a conventional abutment is limited in oral conditions, such as inappropriate location and angle of the fixture and poor thickness of the gum around that (Rieder, 1996). To solve the problems of conventional abutments, with the rapid development of latest computer technology, custom abutment production systems using computer-aided design and computer-aided manufacturing (CAD/CAM) have been introduced to dental clinics (Luthardt, Sandkuhl, Herold, & Walter, 2001; McLaren & Terry, 2002). The abutment production of the CAD/CAM system for dental clinics does not require a casting process that causes casting failure or inappropriateness, which can occur in abutment production, compared to existing casting methods, in the production of the abutment in the casting method. In addition, with the decreasing working hours of the operator, it was reported that the suitability and mechanical properties of the abutment are also excellent (Grossmann, Pasciuta, & Finger, 2006). A custom abutment can give an angle suitable for the oral health status in software or represent an appropriate margin shape in the gingival form, so an ideal upper implant can be produced. In addition, because its production is customized for individuals, an additional emergence profile can be given. Furthermore, the production of aesthetic implants is easy and oral hygiene management is relatively simple, which is good for the health of the surrounding tissues (Heydecke, Sierraalta, & Razzoog, 2002). Because implant prosthesis restorations are generally assembled systems that consist of three elements including upper implant,

abutment and fixture, the mechanical properties of each part change according to the conditions of the connection. Therefore, the transfer of power for each part differs, and there are differences in the joints and the distribution of internal stress of each part. (Wang et al., 2009) A fixture and an abutment are connected through a screw, and the conditions of the connection by the tightening torque can be an important factor affecting implant restoration (Alkan, Sertgöz, & Ekici, 2004). Prosthetic treatment using implants shows an approximately 5-10% failure rate, and it was reported that most cases are accompanied by a screw loosening phenomenon (Jung RE, Pjetursson BE, Glauser, Zembic, Zwahlen, & Lang, 2008), (Jemt, Linden, & Lekholm, 1992). To prevent this phenomenon, it was reported that the stability could be improved by giving an appropriate full weight load when connecting a fixture to an abutment (Jorneus, Jemt, & Carlsson, 1994; Binon, Franz, Brunski, & Gulbransen, 1994; Norton, 1999). The screw tightening torque affects the transfer of power, i.e., stress distribution between a fixture and the cortical bone and between an upper implant and the fixture. If the screw tightening torque is appropriate and the connection between the fixture and abutment is stable, even under the action of masticatory pressure, it would be as solid as the structure of the integrated fixture, and no screw loosening would occur. Similarly, despite the importance of the screw tightening torque in the restoration of implant prostheses, there has been little systematic research on the screw tightening torque of a custom abutment. An effective design, which can disperse an occlusal load during mandible function exercise and the load on the cortical bone, is required (Geng, Tan, & Liu, 2001; Clelland, Ismail, Zachi, & Pipko, 1991; Rieger, Adams, & Kinzel, 1990). Therefore, this study would design an abutment with and aesthetic emergence profile using CAD technology and compare the bio-mechanical difference between the custom abutment and conventional abutment according to the screw tightening torque through 3D finite-element analysis.

2. Materials and Method

2.1 Custom Abutment Design

To design a custom abutment, the proper position of the implant was acquired. For an implant-level impression, the position of the encoded healing abutment was arranged (MyD, RaphaBio, Seoul, Korea). An intraoral scanner (Trios, 3Shape, Copenhagen, Denmark) was used to obtain the scan data of the encoded healing abutment-level. The scan data was entered into the corresponding CAD software (MyD) (Figure 1A). First, using the surface fitting tool, the digital model of the encoded healing abutment and the library data was aligned into the scan body (Figure 1B). The result of the aligned model was obtained (Figure 1C). To obtain a functionally and esthetically proper result, a virtual prosthesis was selected from the authors' library database of artificial teeth (Figure 1D). The virtual artificial teeth were then fixed with CAD software of modification, movement, and rotation (Figure 1E). In addition, the shapes of the custom abutment were designed using the ball control with the recorded step. The long axis of the virtual prosthesis was set as the reference direction. In accordance with the long axis, the convergence angle of the custom abutment was set to 3.75°, and the radius of curvature upon upper angle area was set to 0.7 mm (Figure 1F). The margin was designed as a 1 mm-wide rounded shoulder Figure 1G. Red ball control was used to set the length and width of the anatomical emergence profile design (Figure 1H). To satisfy the individual esthetics and cleaning needs, the cervical margin was set to 0.8–1 mm under an individual gingival margin. Twelve small-sized yellow ball controls were used to adjust the length and the volume of the collars under the cervical margin. This collar design allows the maximum tissue volume and stability of the gingiva. The abutment was also designed according to the natural shape of the prepared teeth (Figure 1I).

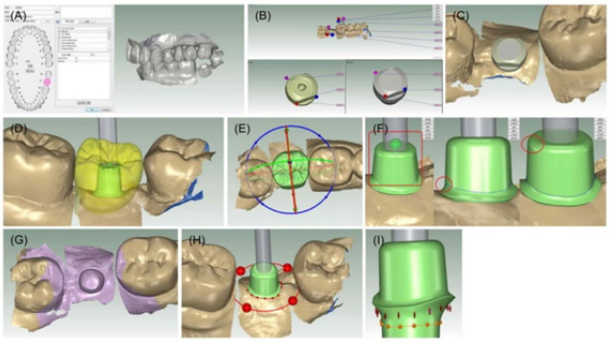

Figure 1. CAD for the custom abutment: (A) Entering the case information and scan data import; (B) Aligning the scanned body; (C) Overlapping of the scanned body; (D), (E) and (F) Setting the location and size of the abutment and the guide of path; (G), (F) Setting the location and the size of the abutment and the path guide; (G) Setting the design of the margin; (H) Setting the primary emergence profile; (I) Designing the abutment collar area

2.2 Finite-Element Model

For the path guide, (I) the abutment axial plane and angle site and (J) the margin and radius of abutment were set. For the cortical bone and cancellous bone of the human body, the entire structure part was assumed to be substances with isotropy, homogenization, and linear elasticity for finite-element analysis by anisotropy or numerical calculations. For modeling and finite-element stress analysis, the finite-element analysis general program, NX 10 (NX10.0.0.24, SIEMENS, Germany) Software was used. After the STL file of the custom abutment produced with the method described above was retrieved in the NX, a reverse design of the custom abutment was carried out using the method for producing the surface based on STL Geometry. Figure 2 shows 3-D images of the custom and conventional abutments. Only differing the shapes of the custom and conventional abutments, the fixture, screw, cortical bone, and cancellous bone were modeled in the same manner. The diameter of the screw was 1.8 mm, and the distance between the screw head and helix was 5.1 mm. In addition, the model employed in this study was a Dio implant system (4.5 mm diameter × 11.5 mm; Dio, Busan, Korea), abutment screw (Ø 1.8 mm × 8.5 mm; Dio), and custom abutment. The abutments, screws, and fixtures used in this study were used to examine the properties of the Ti-6Al-4V material actually produced. Table 1 lists the properties of the material used in this study (Akça & Iplikçioğlu, 2001). The Ti-6Al-4V alloy was reported to have an elastic coefficient of 117.0GPa and a Poisson's.

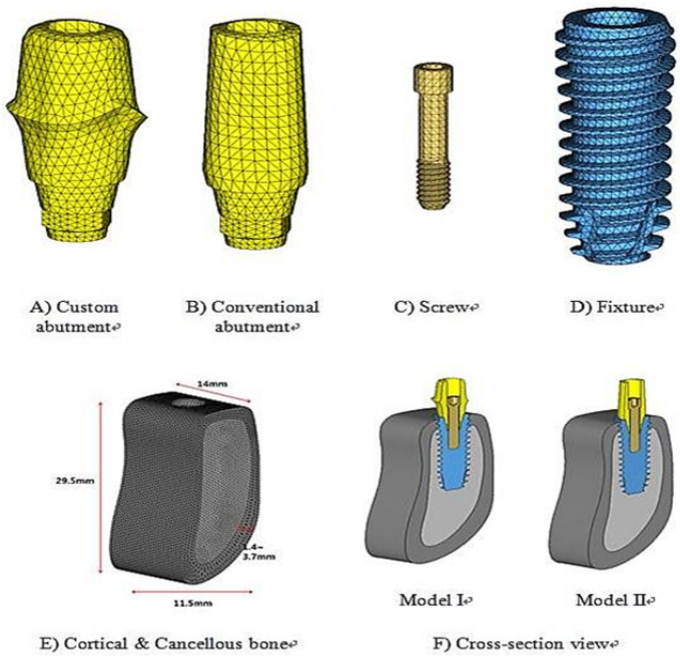

Figure 2. Three dimension analysis structure (Model 1): Custom Abutment, implant and screw in the bone

Ratio of 0.35; its yield strength is 880MPa for Grade 5 and its maximum tensile strength reaches 950 MPa. (Clelland, Ismail, Zachi, & Pipko, 1991), (Jemt, Laney, & Harris, 1991) The cortical bone was modeled in an image, in which the cortical bone with a thickness of 1.4-3.7 mm surrounded the outer angle of the cancellous bone. In contrast, the conventional abutment (4.5 mm diameter × 11.5 mm; Dio, Busan, Korea) was designed by describing the image selling standard. The fixture was implemented with a diameter of 4mm and a length of 13 mm. Figure 2-f shows a section of the 3-D images of the custom and conventional models. The implant was positioned in the cortical and cancellous bone block. Such a configuration allowed a delicate simulation of all models in NX 10 (Siemens PLM Software, Germany). The three-dimensional CAD geometry models was imported into ABAQUS Workbench 6.12 to generate finite elements and perform the numerical simulation. All components were meshed with a 10-node tetrahedron element (mean size: 0.5 mm) using C3D10 type elements readily available in the ABAQUS element library (Table 1).

Table 1. Properties of the materials of the finite element model (Akça & Iplikçioğlu., 2001; Liu, Pearlman, Cooper, Hong, Wang, & Salatin, 2010)

Material		Elastic modulus (GPa)	Poisson ratio
Ti-6AI-4V (abutment, fixture, screw)		117.0	0.35
Supporting Bone	Cortical bone	13.7	0.3
	Cancellous bone	1.85	0.3

Table 2. Quantity of the elements of the finite element model

Material		Element	Shape	Mean Size
Abutment	Custom	4,732	Tetra 10 Node	0.5mm
	Conventional	3,329		
Screw		6,193		
Fixture		21,419		
Supporting Bone	Cortical bone	75,530		
	Cancellous bone	85,114		

2.3 Load and Bond Condition

A perfect bond was presumed because the fixture and cortical bone, and the fixture and screw are combined by the helix, and the fixture and abutment are also combined firmly by the screw tightening torque. On the other hand, a contact condition with a friction coefficient of 0.3 was used on the outside of the screw head and the inside of the abutment. Figure. 3-a shows this boundary condition. As in the Figure, both sides were bonded completely so that no movements to the X-, Y- and Z-axes could be made.

For the screw tightening torque, axial forces that come under 10N·cm, 20N·cm, and 30N·cm were calculated, and it was applied to the middle of the screw head and the helix, as shown in Figure. 3-b. For the screw axial force, the equation 1 (Brown, M, & B. Durbin, 2013) was used and the torque coefficient was assumed to be 0.2. Table 3 lists the calculated axial force.

$$T = KDF \quad (1)$$

where T = tightening torque (N·m), F = axial force (N), D = screw diameter (m), and K = torque coefficient.

A one point force of 175 N was applied 30° oblique to the long axis of the implant coming from the buccal direction. The equivalent stress on the abutment screw caused by the loading conditions were analyzed (Figure. 3-a). (Dong, Kebin, Jiang, Hua, Wenxiu, & Yuyu, 2015)

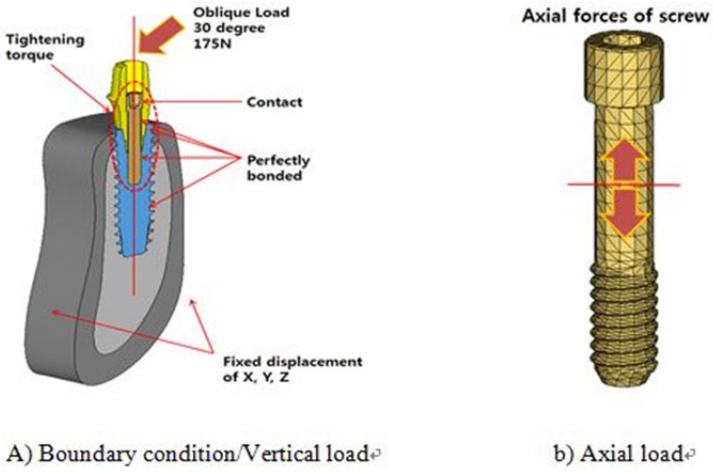

Figure 3. Quantity of the elements of the finite element model

Table 3. Axial force of the screw with regard to the tightening torque of the screw

Tightening torque	Diameter	Torque coefficient	Screw tension
10 N·cm			228 N
20 N·cm	1.8mm	0.2	556 N
30 N·cm			833 N

2.4 Fatigue Analysis

Goodman's fatigue life theory (Budynas & Nisbett, 2008) was reported to be appropriate for a fatigue life evaluation by the static and dynamic loads. (Mahmut & Hasan, 2011)

$$\sigma_\alpha = \frac{\Delta\sigma}{2} = \frac{\sigma_{max}-\sigma_{min}}{2} \quad (2)$$

$$\sigma_m = \frac{\sigma_{max}+\sigma_{min}}{2} \quad (3)$$

$$\frac{\sigma_\alpha}{\sigma_e} + \frac{\sigma_m}{\sigma_u} = \frac{1}{n} \quad (4)$$

Goodman fatigue life theory using the mean stress σ_m and stress amplitude σ_a can be defined as follows: where σ_e is the fatigue limit; σ_u is the maximum tensile strength; and n is the fatigue safety coefficient. The Goodman safety coefficient was calculated, placing the fatigue limit of 510MPa in the above expression when the fatigue cycle of the Ti-6Al-4V material was 10^7 times, as listed in Table 6.

3. Results

3.1 Action of Screw Tightening Torque

By the action of the screw tightening torque, the tensile strength acts in the screw while compression strength acts in the abutment and fixture. Figure 4 shows the section of the custom prosthesis to which 20N·cm was applied, as well as the Max. and Min. Principal. The maximum tensile principal stress appeared in the bottom part of the screw head, and then in the part where the helix began. The maximum compressive stress occurred in the abutment connected to the screw head while in the fixture, it occurred in the part connected to the helix of the screw. In each load and bonding condition of this experiment, the action of the screw tightening torque showed a similar trend in the conventional abutment and custom abutment (Figures of 10N·cm and 30N·cm analysis are attached to the appendix).

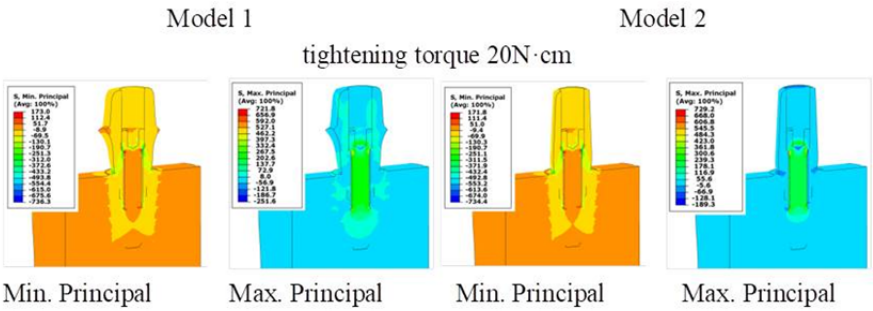

Figure 4. Results of the principal stress with regard to the tightening torque of 20N-cm screw in Models 1 and 2

3.2 Stress Behaviors of Custom/Conventional Abutment Prothesis

Table 4 lists the stress when only the screw tightening torque was applied while no oblique loading was applied. Figure 5 shows the distribution of the custom and conventional stress when the screw tightening torque was 20N·cm. The highest stress occurred in the screw by the screw tightening torque, followed by the abutment and fixture. In addition, the maximum stress on the screw appeared at the bottom part of the screw head. The custom and conventional stress to the screw by the 10N·cm tightening torque were 287.2 MPa and 286.5 MPa, respectively, which are 33% of the yield strength of the material. The screw stress at 20N·cm was 573.9 MPa and 572.4 MPa, respectively, in the custom and conventional abutment, and 65% of the yield strength of the material which is at a slightly lower level than 75%. When a 30N·cm tightening torque was applied, the screw stress was 859.7 MPa and 857.6 MPa in the custom and conventional abutments, respectively, which is approximately 880MPa, the yield strength of Ti-6Al-4V. Figure 6 shows the distribution of the principal stress to the cortical bone when only a 20N·cm tightening torque was applied. For the cortical bone, the Max. and Min. Principal appeared in the opposite part, where the screw of the fixture came into contact with the cancellous bone. For the cancellous bone, Max. and Min. Principal appeared in a similar part in the helix, where it came into contact with the cortical bone. Table 4 shows that the difference in the shape of the custom and conventional abutments had little effect on the Max. and Min. Principal stress on the cortical bone. Table 5 lists the value of the stress of an analysis conducted, assuming the case in which there was no screw tightening torque and a case in which tightening torques of 10N·cm, 20N·cm, and 30N·cm were given and an oblique loading of 175N was applied together. An analysis without the screw tightening torque showed that the maximum stress occurred in the abutment, followed by the fixture and screw.

Table 4. Results of the stress distribution in Models 1 and 2 when applying only the tightening torque of the screw (unit: Mpa)

		10N·cm		20N·cm		30N·cm	
		Model Ⅰ	Model Ⅱ	Model Ⅰ	Model Ⅱ	Model Ⅰ	Model Ⅱ
Abutment (Von Mises Stress)		259.9	258.0	519.3	515.2	778.4	772.1
Screw (Von Mises Stress)		287.2	286.5	573.9	572.4	859.6	857.6
Fixture (Von Mises Stress)		204.3	204.3	408.6	408.5	612.0	612.0
Cortical bone	Max. Principal	1.5	1.5	3.0	3.0	4.5	4.5
	Min. Principal	-2.3	-2.4	-4.7	-4.8	-7.0	-7.1
Cancellous bone	Max. Principal	0.4	0.4	0.9	0.9	1.3	1.3
	Min. Principal	-0.7	-0.7	-1.4	-1.5	-2.1	-2.2

Model 1: custom-abutment implant system

Model 2: conventional-abutment implant system

Table 5. Results of the stress distribution in Models 1 and 2 with regard to the application of a tightening torque and oblique load of the screw (Unit: MPa)

		0		10N·cm		20N·cm		30N·cm	
		Model Ⅰ	Model Ⅱ	Model Ⅰ	Model Ⅱ	Model Ⅰ	Model Ⅱ	Model Ⅰ	Model Ⅱ
Abutment (Von Mises Stress)		274.6	265.1	347.0	334.9	536.9	568.6	822.7	823.7
Screw (Von Mises Stress)		49.2	54.9	309.9	317.6	593.5	601.4	879.7	887.2
Fixture (Von Mises Stress)		168.5	173.4	217.1	217.3	421.1	420.2	624.5	623.6
Cortical bone	Max.Principal	23.5	23.7	24.9	25.1	26.2	26.4	27.5	27.7
	Min.Principal	-35.2	-35.6	-36.6	-37	-37.9	-38.4	-39.1	4.9
Cancellous bone	Max.Principal	4.7	4.7	4.7	4.7	4.8	4.8	4.8	4.8
	Min.Principal	-2.2	-2.2	-2.7	-2.8	-3.3	-3.4	-3.9	-4.0

Model 1: custom-abutment implant system

Model 2: conventional-abutment implant system

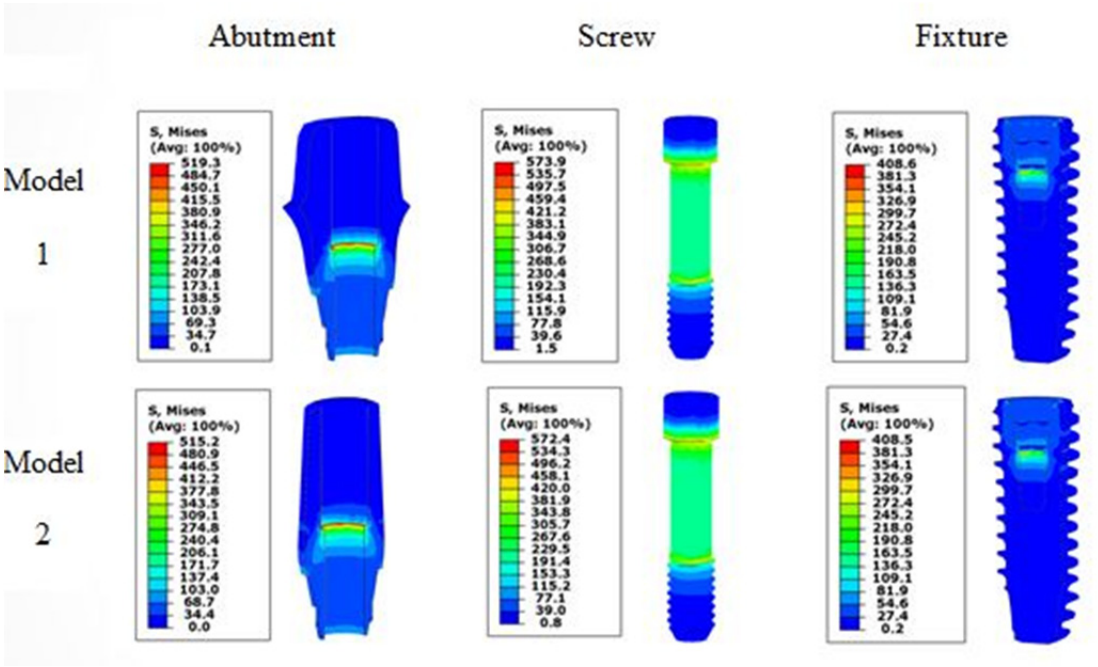

Figure 5. Von Mises stress distribution in Models 1 and 2 with the application of a tightening torque of 20N·cm screw

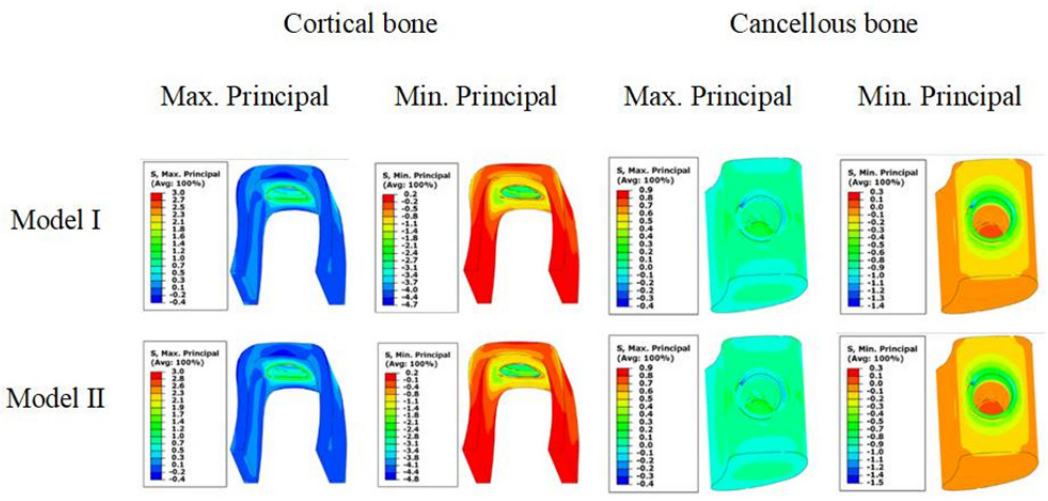

Figure 6. Principal stress distribution of the supporting bone in Models 1 and 2 with the application of tightening torque of a 20N·cm screw

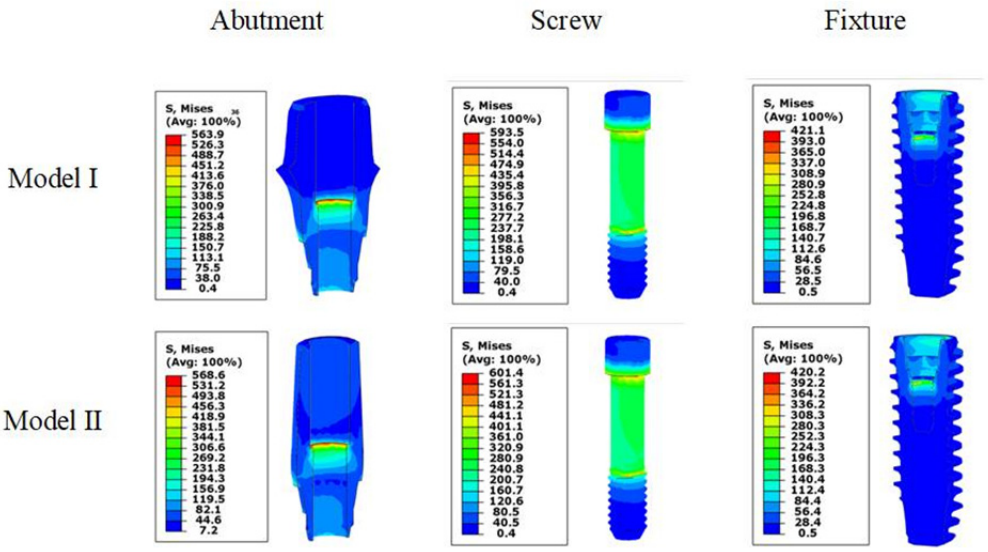

Figure 7. Von Mises stress distribution in Models 1 and 2 with the application of a tightening torque and oblique load of a 20N·cm screw

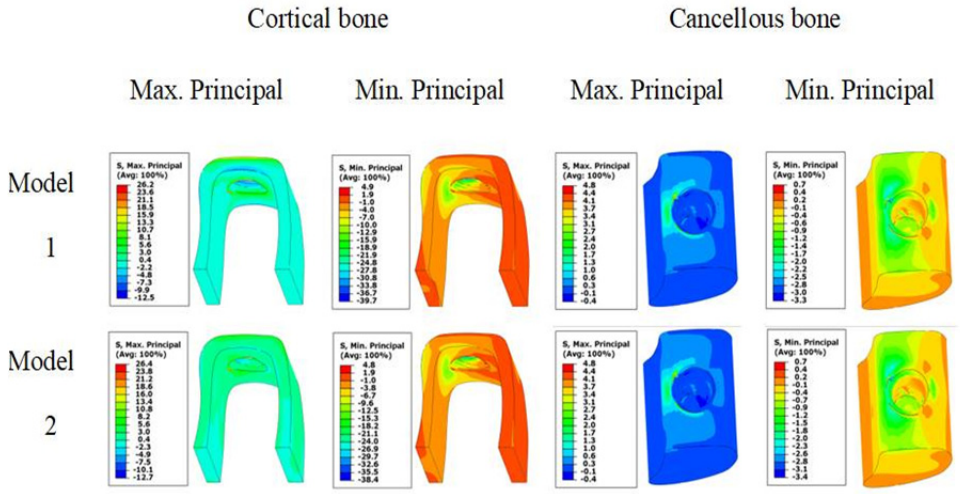

Figure 8. Principal stress distribution of the supporting bone in Models 1 and 2 with the application of a tightening torque and oblique load of a 20N·cm screw

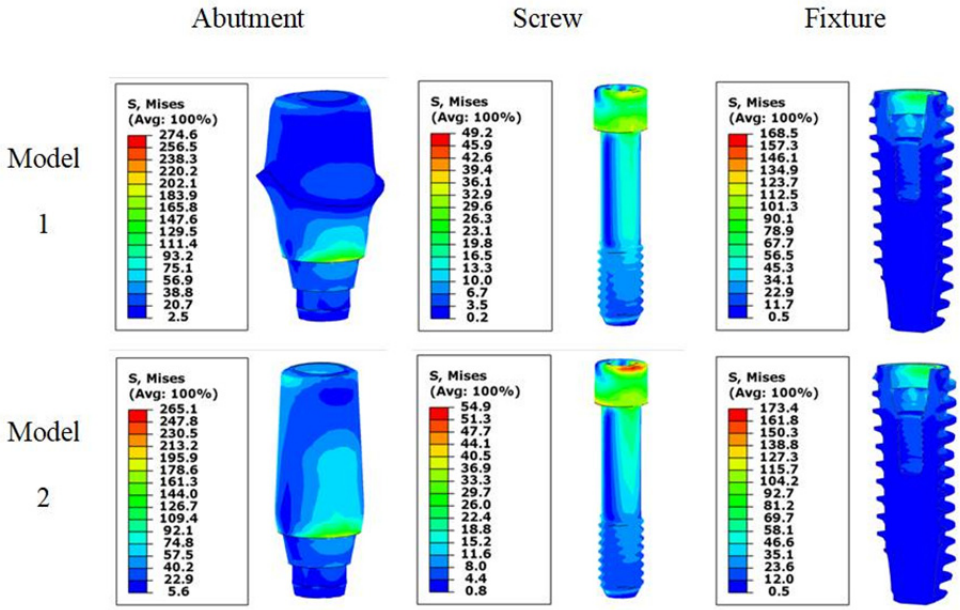

Figure 9. Von Mises stress distribution in Models 1 and 2 with the application of an oblique load when the tightening torque of screw is 0

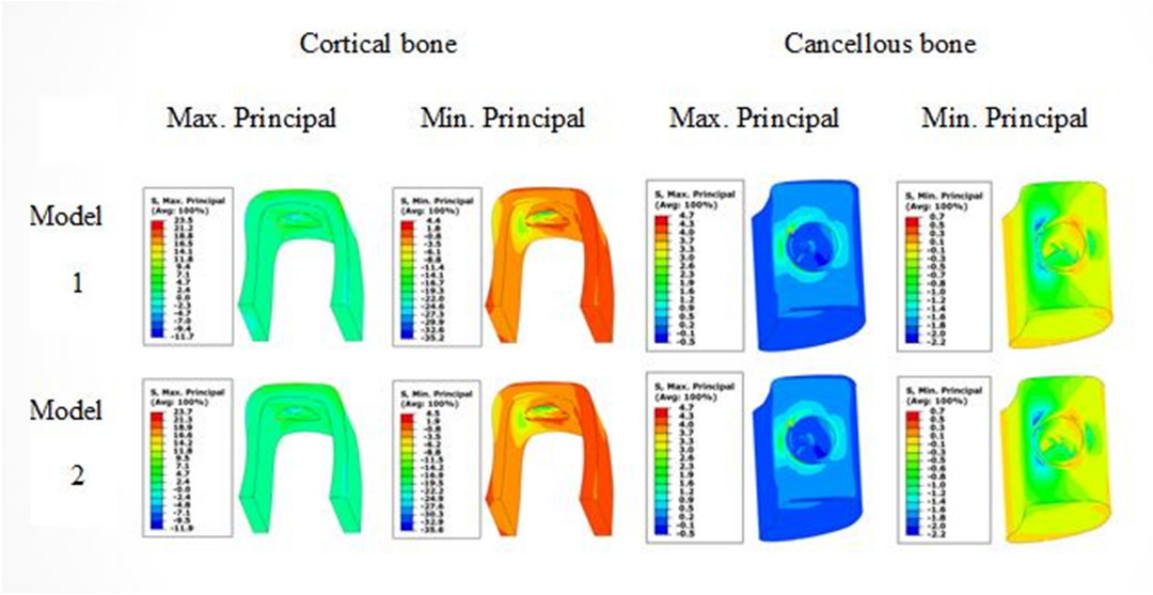

Figure 10. Principal stress distribution of the supporting bone in Models 1 and 2 with the application of an oblique load when the tightening torque of screw is 0

3.2 Fatigue analysis

Based on table 6 for the under oblique load, the highest value of SF occurred at 10N cm. The second level of SF was at 20N cm, which were approximately at the same level. In addition, 30N cm had the third level of SF. The highest value of SF (3.0) was observed at 10N cm. A comparison of the SF of two type models showed a slight difference.

Table 6. Goodman safety factor value of the models in which the tightening torque and oblique load of screw are applied

Classification	10N-cm		20N-cm		30N-cm	
	Model Ⅰ	Model Ⅱ	Model Ⅰ	Model Ⅱ	Model Ⅰ	Model Ⅱ
Abutment	2.5	2.6	1.6	1.6	1.1	1.1
Screw	3.0	3.1	1.6	1.5	1.1	1.1
Fixture	4.4	4.4	2.2	2.2	1.5	1.5

4. Discussion

The aim of this study was to design an abutment with an aesthetic emergence profile using CAD technology and compare the bio-mechanical difference between the custom abutment and conventional abutment according to the condition of the screw tightening torque through a 3D finite-element analysis. In studies conducted previously to utilize the effect of the application of screw tightening torque, a method using the elongation displacement of the screw used by Sakaguchi and Borgersen et al. (Sakaguchi & Borgersen, 1995) and a method using the thermal contraction of the screw used by Alkan et al. (Alkan, Sertgoz, & Ekici, 2004) have been reported. Errors might appear in the research results in situations where abnormal physical conditions are given in the object of analysis, e.g., the screw in the method of screw thermal contraction, while it might be impossible to apply stress in both directions of the structure analyzed using the structure displacement method. Therefore, the tightening torque in this study was implemented so that only the torque would be applied by generating a tensile force as the screw is elongated by the turning force when the screw is connected in the fixture structure and the compressive stress that occurs in the screw head part contacting the inside of the fixture and in the contact interface between the female screw part and the male screw part. The problems raised as demerits of a screw maintenance fixture include that it requires more accurate suitability than a cement fixed type and that there is a reduction of the occlusal area because

of the hole for screw formed in the implant. The greatest clinical issues include loosening of the screw used to maintain and fix the implant and the problem caused by fractures from complex factors, such as the iterative masticatory load, incorrect fitting of the implant, application of a non-functional force, occlusal overload, abnormal occlusal relationship, fixture implant design or the defect of material. (Hebel & Gajjar, 1997; Singer & Serfaty, 1996; Chae, Jong, & June, 1997; Jorneus, Jent, & Carlsson, 1992; Kallus & Bessing, 1994; Haack et al., 1995; Burguete et al., 1994; Naert et al., 1992; Jemt et al., 1991; Rangert et al., 1995; Moon, 2002; Balshi, 1996; W. Becker & B. E. Becker, 1995). From the result of the action of the screw tightening torque (Figure 3-b), the compressive stress appeared in the abutment and fixture around the screw. Therefore, the axial force of the screw tightening torque was properly reflected in the analytical model. The key indicators, such as an abutment, fixture, and screw, were used to judge the fracture of a metal material with ductility to determine if the maximum torsional energy, Von Mises stress has reached the yield strength of the material. On the other hand, because a material with fragility like the cortical bone can judge the fracture through principal stress, this study showed the results of the analysis with the Von Mises stress for the abutment, fixture and screw and with the principal stress for the cortical bone. The maximum tensile stress and compression strength of the cortical bone were 100-130 MPa and 170-190 MPa, respectively, and that both the compressive stress and tensile stress of the cancellous bone should be below 5 MPa so that no fracture occurs. The results of Max. and Min. Principal stress on the cortical bone in Table 4 of this study show a stress below 5MPa, and that there is no large impact of the difference in the shape between the custom and conventional abutment on stress to the cortical bone. According to Paul Binon (Binon et al., 1994), many studies of the screw showed that the tightening torque applied to the screw to prevent loosening is appropriate when it is 75% of the torque that causes the material fracture. The screw is in charge of fixing an abutment to a fixture so that it does not move. On the other hand, screw loosening occurs if the tightening torque is weak, whereas if it is too high, the screw is broken and loses its function as an artificial tooth, and there is great difficulty in removing the helix of the broken screw. Therefore, proper management of the tightening torque is very important. According to the result of an analysis of the screw stress by a 10N·cm tightening torque, it was judged that screw loosening may occur if the masticatory load is conveyed repeatedly to the prosthesis. In contrast, in the 30N·cm one, the screw would be fractured if a strong external power is applied to the prosthesis from dozens to millions of times. In addition, in Table 5, as a result of the analysis, assuming a case in which no screw tightening torque was applied and a cases in which 10N·cm, 20N·cm, and 30N·cm full weight loads were applied with an oblique loading, when screw tightening torque was not applied, the maximum stress occurred in the abutment, followed by the fixture and screw. This tends to be different from the case, in which screw tightening torque was applied, and considering that the damage on implants occurs mostly in the screw in the clinic, it was judged that the cause for the occurrence in the clinic was not detected appropriately. In the results of the 20N·cm screw tightening torque and oblique loading in Table 5, the screw stress of Model 1 was 7.9 Mpa lower than that of Model 2 and the fixture was 0.9 MPa higher. The difference was within 1.5% of the total stress, but a custom abutment is better than a conventional one considering that a loss of function by prosthetic fracture occurs mostly in the screw. The difference between the custom and conventional abutments had little effect on the cortical bone. The Max.and Min. Principal stress on the cortical bone summarized in Table 5 is within the fracture criterion mentioned above, and there was almost no difference between the two models. In addition, fracture can occur in a metal material, even below the yield strength by the iterative load, which is called fatigue fracture. (Shackelford & James, 2005) This should be considered together because in a prosthesis, the screw tightening torque, static load and external force, dynamic load act simultaneously.

Table 6 lists the safety factor of custom implant system with three different tightening torques under the loading condition of oblique. The SF is often calculated based on the yield stress over the design stress. The minimum criterion value of the SF was assumed to be 1, which explains why the load generated in the structure reaches the failure limitation. All results of the safety coefficient exceeded the critical mass safety coefficient 1.0 that could endure a 175N oblique load 10 times. On the other hand, since the Goodman's safety coefficient of architectures or main machine parts is designed to be higher than 2.0-2.5, it was judged to be necessary to secure a safety coefficient at least about 1.5 for the prosthesis. Therefore, it is appropriate to determine the screw tightening torque around 20N·cm. The limitations of this study include the differences in the homogenization and isotropy of the cortical bone, which were set up as the initial hypotheses, and the actual occlusal force in the human body is a dynamic load, which is different from the static load in the duration and size of stress, so it is necessary to conduct studies of more precise material properties, model composition, and load application. In addition, because the parameter value of the custom abutment in a form limited to some patients was used, it is essential to conduct a study that can set up clinically allowable category guidelines in designing custom abutment in the future.

5. Conclusion

This study examined the stress behaviors of custom and conventional prostheses by an external load, and the following conclusion was obtained. *The screw tightening torque affected the changes in the stress* of the abutment, screw, and fixture. The status, in which the screw load was applied, described more realistic prosthesis fracture behavior than the one in which it was not. With the finite-element model used in this study, the appropriate screw tightening torque showed a stable stress dispersion when a 20N·cm screw tightening torque was applied more than when 10N·cm and 30N·cm ones were applied. The difference between the custom and conventional abutment has little effect on the cortical bone by the external load. Less screw fracture occurred in the custom abutment because the stress occurring in the screw showed a lower result in the custom abutment than in the conventional one.

Acknowledgments

This study was supported by the Institute for Information & Communications Technology Promotion (IITP) grant funded by the Korea government (MSIP) (B0101-16-1081, Development of ICT based software platform and service technologies for medical 3D printing applications

Competing Interests Statement

The authors declare that there are no competing or potential conflicts of interest.

References

Akça, K., & Iplikçioğlu, H. (2001). Finite element stress analysis of the influence of staggered versus straight placement of dental implants. *Int J Oral Maxillofac Implants, 16*, 722-730.

Alkan, I., Sertgoz, A., & Ekici, B. (2004). Influence of occlusal forces on stress distribution in preloaded dental implant screws. *J Prosthet Dent., 91*(4), 319-325. https://doi.org/10.1016/j.prosdent.2004.01.016

Balshi, T. J. (1996). An analysis and management of fractured implants: a clinical report. *Int J Oral maxillofac Implants, 11*(5), 660-666.

Becker, W., & Becker, B. E. (1995). Replacement of maxillary and mandibular molars with single endosseous implant restorations: A retrospective study. *J Prosthet Dent., 74*(1), 51-55. https://doi.org/10.1016/S0022-3913(05)80229-X

Bichacho, N. (1998). Achieving optimal gingival esthetics around restored natural teeth and implants. Rationale, concepts, and techniques (Vol. 42, pp.763-780). Dental Clinics of North America.

Binon, P., Franz, B. J., & Gulbransen, H. (1994). The role of screws in implant systems. *Int J Oral Maxillofac Implants, 9*, 48-63.

Binon, P., Sutter, F., Beaty, K., et al. (1994). Cement-retained versus screw-retained implant restorations: achieving optimal occlusion and esthetics in implant dentistry. *Int J Oral Maxillofac Implants, 9*(supplement), 48-63.

Brown, M., & Durbin, B. (2013), Guideline for Bolted Joint Design and Analysis: Version 1.0." Sandia Report, SAND2008-0371. *Sandia National Laboratories for United States Dept. of Energy,* (12), 2013.

Budynas, R. G., & Nisbett, J. K. (2008). *Shingles's Mechanical Engineering Design: 9Th*.

Burguete, R. L., Johns, R. B., King, T., et al. (1994). Tightening characteristics for screwed joints in osseointegrated dental implants. *J Prosthet Dent., 71*(6), 592-599. https://doi.org/10.1016/0022-3913(94)90443-X

Chae, H. C., Jong, Y. S., & June, K. L. (1997). Cement - retained versus screw - retained implant restoration. *Oral Biology Research, 21*(1), 149-158.

Clelland, N. L., Ismail, Y. H., Zachi, H. S., & Pipko, D. (1991). Three dimensional finite element stress analysis in and around the screw-vent implant. *Int J Oral Maxillofac Implants, 6*(4), 391-398.

Dong, W., Kebin, T., Jiang, Ch., et al. (2015). A Further Finite Element Stress Analysis of Angled Abutments for an Implant Placed in the Anterior Maxilla. *Computational and Mathematical Methods in Medicine*. http://dx.doi.org/10.1155/2015/560645

Geng, J. P., Tan, K. B., & Liu, G. R. (2001), Application of finite element analysis in implant dentistry: a review of the literature. *J Prosthetic Dent., 85*(6), 585-598.

Grossmann, Y., Pasciuta, M., & Finger, I. M. (2006). A novel technique using a coded healing abutment for the fabrication of a CAD/CAM titanium abutment for an implant-supported restoration. *J Prosthet Dent., 95*,

258-261.

Haack, J. E., Sakaguchi, R. L., Sun, T., et al. (1995). Elongation and preload stress in dental implant abutment screws, *Int J Oral Maxillofac Implant, 10*(5), 529-536.

Hebel, K. S., & Gajjar, R. C. (1997). Cement-retained versus screw-retained implant restorations: achieving optimal occlusion and esthetics in implant dentistry., *J Prosthet Dent., 77*(1), 28-35.

Heydecke, G., Sierraalta, M., & Razzoog, M. E. (2002). *Evolution and use of aluminum oxide single-tooth implant abutments: a short review and presentation of two cases* (Vol.15, pp.488-93).

Jemt, T., Laney, W. R., Harris, D., et al. (1991). Osseointegrated implants for single tooth replacement: a 1-year report from multicenter prospective study. *Int J Oral Maxillofac Implants, 6*(1), 29-36.

Jemt, T., Linden, B., & Lekholm, U. (1992). Failures and complications in 127 consecutively inserted fixed prostheses supported by Brånemark implants. *From prostheses treatment to first annual check up*. *Int J Oral Maxillofac Implants, 7*, 40-3.

Jorneus, L., Jemt, T., & Carlsson, L. (1994). Loads and designs of screw joints for single crowns supported by osseointegrated implants. *Int J Oral Maxillofac Implants, 7*, 353-9.

Jorneus, L., Jent, T., & Carlsson, L. (1992) Loads and designs of screw joint for single crowns supported by osseointegrated implants. *J Prosthet Dent., 7*(3), 353-359.

Jung, R. E., Pjetursson, B. E., Glauser, R., Zembic, A., Zwahlen, M., & Lang, N. P. (2008), A systematic review of the 5-year survival and complication rates of implant-supported single crowns. *Clin Oral Implants Res., 19*, 119-30.

Kallus, T., & Bessing, C. (1994). Loose gold screws frequently occur in full-arch fixed prostheses supported by osseointegrated implant after 5 years. *Int J Oral Maxillofac Implants, 9*(2), 169-178

Liu, H. Y., Pearlman, J., Cooper, R., et al. (2010). Evaluation of aluminum ultralight rigid wheelchairs versus other ultralight wheelchairs using ANSI/RESNA standards. *Journal of rehabilitation research and development, 47*(5), 441-456. https://doi.org/10.1682/JRRD.2009.08.0137

Luthardt, R. G., Sandkuhl, O., Herold, V., & Walter, M. H. (2001), Accuracy of mechanical digitizing with a CAD/CAM system for fixed restorations. *Int J Prosthodont, 14*, 146-51.

Mahmut, P., & Hasan, Y. (2011). Comparison of fatigue behaviour of eight different hip stems: a numerical and experimental study. *J. Biomedical Science and Engineering, 4*, 643-650 https://doi.org/10.4236/jbise.2011.410080

McLaren, E. A., & Terry, D. A. (2002), CAD/CAM systems, materials and clinical guidelines for all-ceramic crowns and fixed partial dentures. *Compend Contin Educ Dent., 23*, 637-41.

Moon, T. C. (2002). A literature review on the survival rate of single implant - supported restorations. *Jounal of Periodontal & Implant Science, 32*(1), 69-87.

Naert, I., Quirynen, M., Van Steenberghe, D., et al. (1992). A six-year prosthodontic study of 509 consecutively inserted implants for the treatment of partial edentulism. *J Prosthet Dent., 67*(2), 236-245. https://doi.org/10.1016/0022-3913(92)90461-I, https://doi.org/10.1097/00008505-199200140-00015

Norton, M. R. (1999). Assessment of cold welding properties of the internal conical interface of two commercially available implant systems. *J Prosthet Dent., 81*, 159-66.

Rangert, B., Krogh, P. H. J., Langer, B., et al. (1995). Bending overload and implant fracture: a retrospective clinical analysis. *Int J Oral Maxillofac Implant, 10*(3), 326-334

Rieder, C. E. (1996). *Customized implant abutment copings to achieve biologic, mechanical, and esthetic objectives*. *Int J Periodontics Restorative Dent, 16*, 20-9.

Rieger, M. R., Adams, W. K., & Kinzel, G. L. (1990). A finite element survey of eleven endosseous implants. *J Prosthet Dent., 63*(4), 457-465.

Sakaguchi, R., & Borgersen, S. E. (1995). Non-linear contact analysis of preload in dental implant screws. *Int J Oral Maxillofac Implants, 10*(3), 295-302

Singer, A., & Serfaty, V. (1996). Cement-retained implant-supported fixed partial denture: a 6-month to 3-year follow-up. *Int J Oral Maxillofac Implants, 11*(5), 645-659.

Ting, W., Wenhe, L., Ning, D., & Chunbo, T. (2010). Design of a custom angled abutment for dental implants using

computer-aided design and nonlinear finite element analysis. *Journal of Biomechanics, 43*, 1941-20. https://doi.org/10.1016/j.jbiomech.2010.03.017

Wang, R. F., Kang, B, Lang, L. A., & Razzoog, M. E. (2009). The dynamic natures of implant loading. *Prosthet Dent., 101*, 359-71.

Welsch, G., Boyer, R., & Collings, E. W. (Eds.) (1993). *Materials properties handbook: titanium alloys*. ASM international.